Null-space Monte Carlo particle tracking to assess groundwater PCE (Tetrachloroethene) diffuse pollution in north-eastern Milan functional urban area

Luca Alberti [a], Loris Colombo [a,*], Giovanni Formentin [b]

[a] Politecnico di Milano, DICA Dipartimento di Ingegneria Civile e Ambientale, P.zza Leonardo da Vinci 32, 20133 Milano, Italy
[b] Tethys srl, Viale Lombardia 11, 20131 Milano, Italy

ABSTRACT

The Lombardy Region in Italy is one of the most urbanized and industrialized areas in Europe. The presence of count-less sources of groundwater pollution is therefore a matter of environmental concern. The sources of groundwater contamination can be classified into two different categories: 1) Point Sources (PS), which correspond to areas releas-ing plumes of high concentrations (i.e. hot-spots) and 2) Multiple-Point Sources (MPS) consisting in a series of unidentifiable small sources clustered within large areas, generating an anthropogenic diffuse contamination. The latter category frequently predominates in European Functional Urban Areas (FUA) and cannot be managed through standard remediation techniques, mainly because detecting the many different source areas releasing small contam-inant mass in groundwater is unfeasible. A specific legislative action has been recently enacted at Regional level (DGR IX/3510-2012), in order to identify areas prone to anthropogenic diffuse pollution and their level of contamination. With a view to defining a management plan, it is necessary to find where MPS are most likely positioned. This paper describes a methodology devised to identify the areas with the highest likelihood to host potential MPS. A ground-water flow model was implemented for a pilot area located in the Milan FUA and through the PEST code, a Null-Space Monte Carlo method was applied in order to generate a suite of several hundred hydraulic conductivity field realizations, each maintaining the model in a calibrated state and each consistent with the modelers' expert-knowledge. Thereafter, the MODPATH code was applied to generate back-traced advective flowpaths for each of the models built using the conductivity field realizations. Maps were then created displaying the number of backtracked particles that crossed each model cell in each stochastic calibrated model. The result is considered to be representative of the FUAs areas with the highest likelihood to host MPS responsible for diffuse contamination.

* Corresponding author.
E-mail address: loris.colombo@polimi.it (L. Colombo).

Published Journal Article available at: https://doi.org/10.1016/j.scitotenv.2017.11.253

1. Introduction

Stating that groundwater is the most sensitive and the largest body of freshwater in the European Union and the main source of public drinking water supplies in many regions, the European Community in 2006 (European Union, 2006) established some measures in order to prevent and control groundwater pollution. One of the main aim of the Community (European Environment Agency, 2013) has been to issue rules for groundwater management and to identify point source contaminations as the first step toward remediation. Point sources (PS) can be defined as contamination hot spots releasing plumes with high concentrations. Nevertheless, in many urbanized areas, contami-nant plumes originated by single point sources frequently overlap with a widespread contamination caused by multiple-point sources (MPS). These are made up of a series of unidentifiable small sources clustered in a large area, generating a diffuse contamination not ascrib-able to a unique known source. These areas cannot be remediated by re-course to standard remediation techniques, mainly because: a) the identification of MPS is difficult or impossible by virtue of their small mass release and b) the wide extension of the contaminated areas. Therefore, the design of alternative remediation approaches beforehand requires methods to assess the presence of a diffuse contamination and methods to distinguish point source (PS) and multiple-point source (MPS) contribution.

Kuroda and Fukushi (2008) observed that urban areas are the most important MPS of groundwater contamination due not only to the small number of big industries, but also to the large number of residents, whose collective actions bring about serious consequences. The extension of sewage system networks and the inadequateness of old sewer systems to cope with the increased effluent load represent some major causes (Nolan et al., 2002; Stevenazzi et al., 2015, 2017). Further-more, other forms of urban MPS pollution include roadways, parkings and other surfaces of improperly managed construction sites from which oil, grease and toxic chemicals can be released (Frumkin, 2002).

Recently, a new statistical methodology has been developed in order to assess anthropogenic diffuse contamination in Functional Urban Areas (Alberti et al., 2016a). However, once the areas prone to diffuse contamination are defined, in order to plan the groundwater resource management it is still necessary to identify the areas most likely to con-tain the MPS. In the last 20 years, a large amount of methods were tested and developed to identify PS: Integral Pumping Tests (Alberti et al., 2003, 2011; Bauer et al., 2004; Bayer-Raich et al., 2006) and inverse transport modeling (Carrera et al., 2005; Citarella et al., 2015; Zhang et al., 2016). Unfortunately, few methods have been developed to iden-tify anthropogenic diffuse contamination sources. Nevertheless, the identification of areas most likely to host potential MPS and the assess-ment of their strength is an issue of primary importance, and in this study it has been addressed through the help of groundwater modeling. The approach is that of inverse modeling, by which measurements of system variables provide the information required to identify the system parameters governing the flow equation.

In Functional Urban Areas (FUA), the frequent presence of a diffuse contamination by chlorinated hydrocarbons is the result of a wide-spread use of these substances in many different production activities since the 1940s (Provincia di Milano, 1992). Transport of these contam-inants in groundwater depends on many variables, such as hydraulic conductivity, dispersivity, position and magnitude of sources. The un-certainties inherent in the link between source characteristics (position and magnitude) and concentration measurements make it impossible to unequivocally identify all the sources. Thus, a probabilistic frame-work allowing to quantify the uncertainties in the position of contami-nant sources responsible for a diffuse contamination should be adopted. For this purpose, the present paper focuses on the uncertainty of the hy-draulic conductivity distribution and consequently of the groundwater flow direction that conditions the advective component in the transport of contaminants (Pollock, 1994, 2012).

The problem of non-unique groundwater flow solution has been ad-dressed by many authors. Carrera and Neuman (1986) discussed how non-unique inverse problems can be solved in an underdetermined context. In terms of hydrogeological reliability, parameter sets should then be used to estimate model predictions of interest. Therefore, the uncertainty of each model prediction can be characterized by a proba-bility density function with a mean, which is the approximation to the prediction of minimum error variance, and a standard deviation that provides the uncertainty of the model prediction (Herckenrath et al., 2011). Several methods are available for quantifying uncertainty in pre-dictions by use of a calibrated model (Tonkin and Doherty, 2009): linear methods are applied with a variance propagation both in the traditional overdetermined inverse modeling and in the underdetermined context (Bard, 1974; Draper and Smith, 1981; Moore and Doherty, 2005). Non-linear methods of predictive uncertainty were described by Christensen and Cooley (1996).

The Null-Space Monte Carlo (NSMC) analysis provides a mechanism for the exploration of the uncertainty associated to measurement error, enabling the model to fill the observed data with a suitable stochastic descriptor of parameter variability within the study area. The classical methods such as likelihood uncertainty estimation (Beven and Binley, 1992) are difficult to use in highly parameterized models, especially in solute transport models. There are several examples of constrained Monte Carlo analysis in the groundwater context (Carrera et al., 2005; Guadagnini and Neuman, 1998; Harvey and Gorelick, 1995), but the high computational effort of the model decreases the applicability of these methods. Tonkin and Doherty (2009) presented a new method that achieves efficient production of a multitude of calibration-constrained stochastic parameter fields.

As Northern Italy is one of the most relevant urbanized and industri-alized areas in Europe, it hosts a large number of sources of contamina-tion that affect groundwater quality. These facts, together with the availability of a large number of field data and a wide quantity of studies, offer the possibility of finding useful pilot areas for the analysis of diffuse contamination. In this paper, the NSMC methodology is applied and tested in a pilot area in the N-E sector of Milano FUA, where many hydrogeological and chemical data have been collected at different loca-tions over thirty years. The procedure aims at identifying the potential source areas of diffuse contamination taking into account the uncer-tainties tied to the dynamics of the advective solute transport in groundwater. Therefore, the purpose of this work is not to identify the exact source positions but rather to identify locations with an associated occurrence frequency where MPS may contribute to PCE concentrations measured in groundwater samples that exceed the Italian Decree Law (31/2001) drinking-water standard of 10 μg/l.

1.1. Site hydrogeology and groundwater deterministic flow model

The modeled area is located in the Lombardy Region (Fig. 1), within the Po Plain, and it includes the North-Eastern sector of Milan city and some surrounding municipalities. The area is 120 km^2 wide, lies at the center of one of the most urbanized and industrialized areas in Europe and is affected by groundwater contamination caused either by some known plumes or by diffuse pollution. The central part is occupied by a former steel plant, which had been active during most of the last century. The area has been subjected to characterization and reclama-tion since the '90s, hence a significant number of stratigraphic, hydrogeological and concentration data are available covering a period of about thirty years.

Some sectors of the Pilot Area are highly contaminated by chlorinated hydrocarbons (mainly PCE and TCE) and Chromium VI. Thanks to recent investigations funded by Regione Lombardia (ARPA Lombardia, 2016) it has been possible to separate the plumes linked to PS from a diffuse con-tamination linked to MPS (Alberti et al., 2016a). Through a multivariate statistical approach combined with transport modeling, a diffuse PCE contamination has been identified (Fig. 2 and Fig. S1) with average

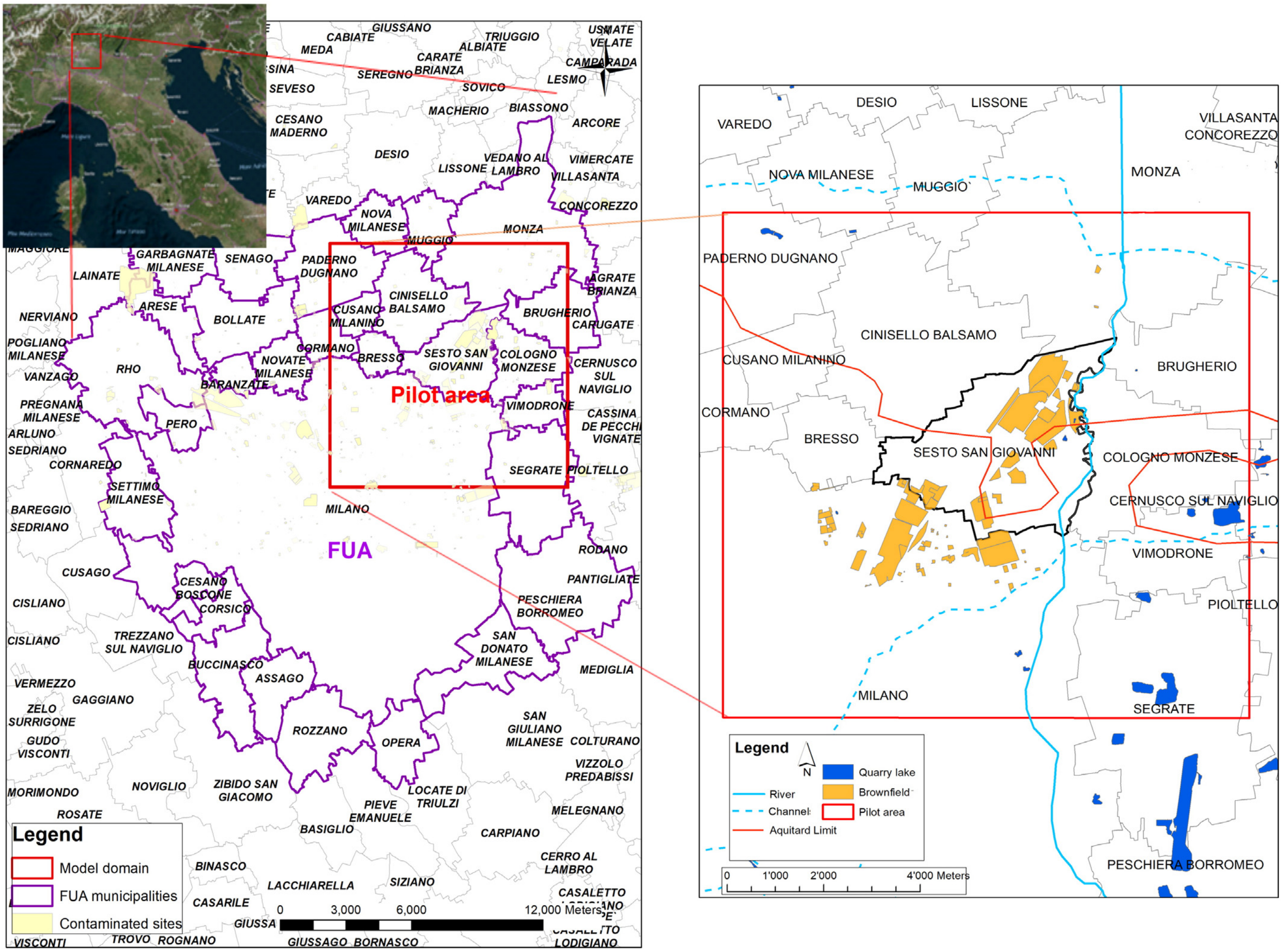

Fig. 1. a) Functional Urban Area (31 municipalities extended for 486 km^2) and b) pilot area (red square): the domain is extended 120 km^2, main brownfields are centered on the domain.

concentrations varying from 2.9 µg/l (within the yellow zone) to 18.1 µg/l (within the red zone).

The main aquifers in the Lombardy Plain are hosted by a sequence of plio-pleistocenic sediments that filled the Neogene Po plain foredeep reaching a maximum thickness of approximately 500 m (Bini, 1997; Carcano and Piccin, 2002; Perego et al., 2014). At the base of the se-quence, pelagic sediments are mainly clay and silt. At the top, gravel and sand are predominant and fed the basin under the control of Middle to Late Pleistocene glacial cycles. The origin of the latter is alluvial and glacio-fluvial, and the hosted aquifers reveal the highest transmissivity values. Four main aquifers (named from A to D) are recognized in the Lombardy Plain, but only three were extensively investigated through drillings in the Milan area (Alberti et al., 2014; Alberti et al., 2016a, 2016b; Alberti and Francani, 2001; Francani and Beretta, 1995; Gattinoni and Scesi, 2017; Pedretti et al., 2013). The case study discussed here focuses only on aquifers A and B, which in the Southern part of the domain are separated by a clay layer (aquitard) that becomes discontinuous and then disappear Northwards (Fig. 2 and Fig. 3).

The deterministic groundwater flow model was previously implemented through MODFLOW-2000 (Harbaugh et al., 2000) in the PLUMES project funded by the Lombardy Region (ARPA Lombardia, 2015), and is used in this paper to build the stochastic flow model with NSMC procedure. In this section, the site-specific deterministic model is briefly discussed.

The flow model is made up of three layers, each of them uniformly divided into square cells 50 m wide, for a total of 219 rows and 218 columns. While the total covered area is approximately 120 km^2, the area of interest is smaller (about 1/3) and it is located at the center of the model domain corresponding to the Sesto San Giovanni municipality (Fig. 4). The first model layer has an average thickness of 30 m and represents the shallow aquifer (Aquifer A). The hydraulic conductivity ranges between $1\cdot10^{-5}$ and $4\cdot10^{-3}$ m/s. The aquitard lies at an average depth of about 40 m and is represented by the second layer with an average thickness of 5 m and an hydraulic conductivity that, from South to North, varies from low values ($1\cdot10^{-9}$ m/s) to sand and gravel values ($1\cdot10^{-3}$ m/s) where the clay lens disappear (aquitard boundary is the red line in Fig. 2). This allows for the representation of the pinch-out of the clay layer and the presence of a unique aquifer in the northern part of the domain. Underneath, a second aquifer (Aquifer B) is present and partially separated from the shallow one. This aquifer is represented by the third layer with a hydraulic conductivity varying between $1\cdot10^{-5}$ and $1.5\cdot10^{-3}$ m/s and an average thickness of 60 m. Boundary conditions (Fig. 4) were computed from piezometric surface maps generated from the hydraulic head survey of May 2014 (showed in Fig. 2 a and b). Constant heads are deemed suitable as the previous piezometric campaigns showed a stable direction of the groundwater flow and the area of interest lies at the center of the model domain at a distance of 4.5 km from boundaries (Fig. 4). Internal boundary conditions represent rivers, irrigation channels and groundwater withdrawals. The MODFLOW RIVER package has been used to represent the Lambro river, the levels of which were measured during May 2014 and geometry characteristics were gathered from public documents. Two main irrigation channels (Villoresi and Martesana) are represented through the WELL package (Fig. 4) in order to consider their constant leakage

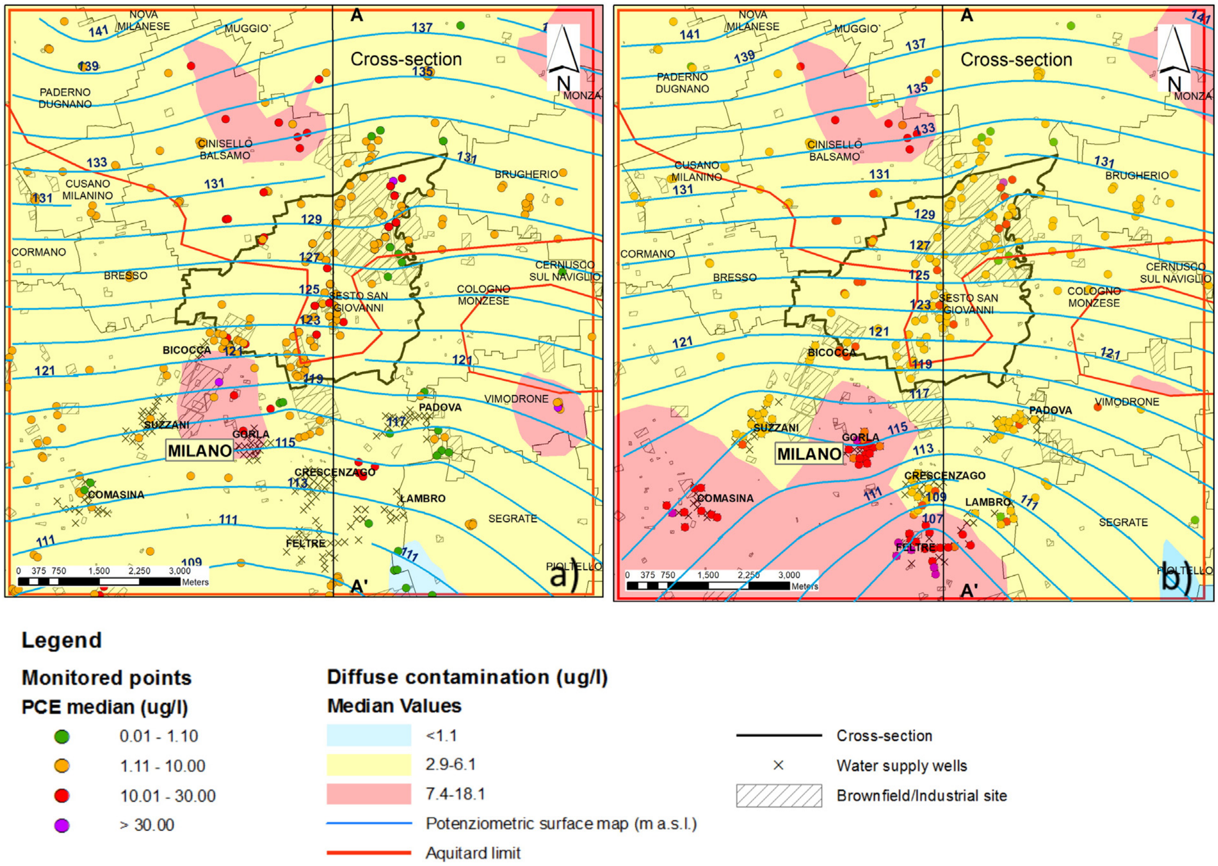

Fig. 2. The figure shows the median PCE concentration data at each monitoring wells (derived from the ARPA database, 2010–2014), the diffuse contamination map (ARPA Lombardia, 2016) and the groundwater head monitored in May 2014 for a) shallow aquifer (Aquifer A) and b) semi-confined/confined aquifer (Aquifer B).

into the aquifer: using data shared by the irrigation Consortium the inflow was calculated as the total water loss at the bottom of the channel stretched within the domain. Public and private withdrawals (Fig. S2) are inserted as constant outflows based on information gathered at the local public water utilities and at Regione Lombardia. Finally, surfi-cial recharge to the aquifer system for spring 2014 was simulated using the RECHARGE package with values calculated as the sum of re-charge from precipitation and from the secondary irrigation channel network (Alberti et al., 2016; Alberti and Francani, 2001). The latter one does not account for the leakage from the bottom of the two main channels (which is represented through the WELL package), but only the amount of water that is distributed on crop fields by the secondary channel network. Recharge from precipitation was estimated by the Thornthwaite method (Thornthwaite and Mather, 1955) and distributed based on land use and land cover (Fasolini and Zini, 2014). Recharge from secondary irrigation channels was calculated based on the irriga-tion network and flow data provided by the Irrigation Consortium (Consorzio Villoresi).

As stated above, the model was previously calibrated in a deterministic way with the iterative parameter estimation software package (PEST), implemented in the Modflow Windows graphical interface GWV6 (Doherty, 2010, 2014; Doherty et al., 2005; Rumbaugh and Rumbaugh, 2014). A set of 63 water levels, measured in May 2014, were used, in accordance with Doherty and Welter (2010), to calculate the objective function as in Eq. (1). PEST aims at minimizing the objective function adopting the gradient-based Gauss-Marquardt-Levenberg algorithm. At the end of the process, the model reached a good fit to measurements with an absolute residual mean of 0.16 m and a scaled absolute residual mean of 0.3% (Fig. S3, Table S1).

A groundwater model typically represents a complex natural system with a set of mathematical equations and boundary conditions (BCs) that describe the main processes governing groundwater flow. In addition to some intrinsic errors (assumptions and simplifications overall), hydrogeologic errors are a combination of errors mainly based on estimation of hydrogeologic parameters, recharge and BCs during the calibration procedure (Troutman, 1985). Furthermore, close agreement between simulated and measured values does not guarantee that the estimated parameter values (in this case hydraulic conductivities) represent a unique parameter set. Alternate hydraulic conductivity combinations may generate model calibration results that are equally valid and should be considered through a stochastic approach.

2. Methodology

The proposed methodology has been developed during the PLUMES regional projects (2015–2016) and further during and the European project AMIIGA (Interreg Central Europe, CE32 2017–2019), which among the outputs has the aim to create effective tools for Public Authorities useful to develop groundwater management plans in FUAs affected by diffuse contamination.

Starting from the deterministic calibrated model, a process called Null-Space Monte Carlo (NMSC) is used to randomly generate 400 different realizations of hydraulic conductivity (K) fields, all of which provide a satisfactory fit to observations. The variability in the K- fields reflects the uncertainty with which the system is known and represented by the model; this variability translates into differences in the distribution of simulated heads, hence in the paths followed by the contaminants. As determining the likely position of small distributed sources (i.e. MPS) that are responsible for diffuse contamination is the main

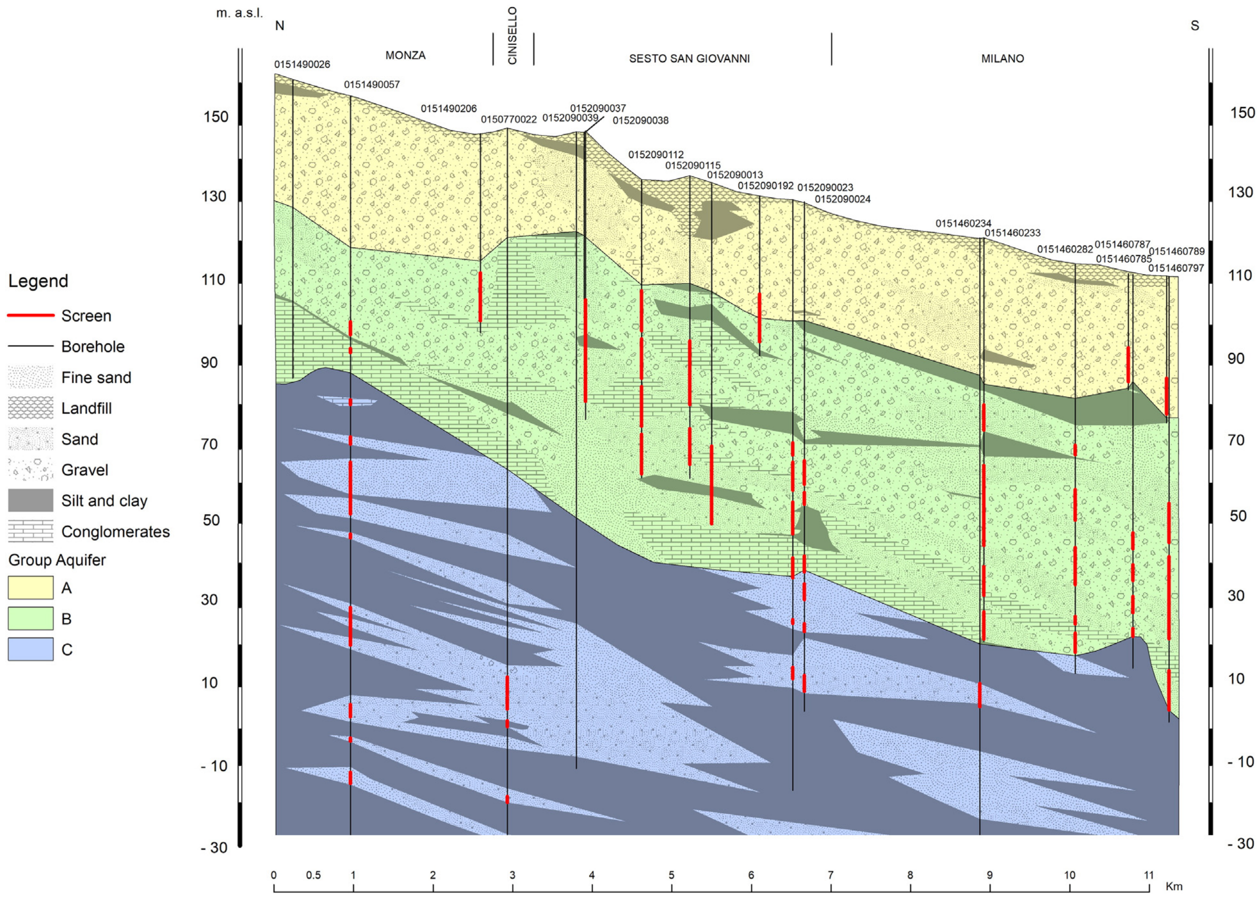

Fig. 3. Hydrogeological cross-section N-S of the pilot area corresponding to line A-A' of Fig. 2.

focus of this study, a calibration-constrained Monte-Carlo analysis combined with particle back-tracking (MODPATH version 5) has been used to explore the uncertainty governing the particle pathlines, which in turn is associated with the position of MPS. The purpose of calibration-constrained Monte-Carlo analysis is therefore to generate a suite of pa-rameter field realizations that express the variability in the particle paths (which in turn represent the advective paths followed by contam-inants in groundwater) as a function of the uncertainty in model param-eters. Each of the different parameter sets generated in the Monte-Carlo procedure is subjected to the constraint that model outputs provide a good match with their respective observations (i.e. head targets). Calibration-constrained parameter field generation was implemented using the Null-Space Monte Carlo (NSMC) method described by Herckenrath et al. (2011) and Tonkin and Doherty (2009), and imple-mented in the PEST package (Doherty, 2010, 2014; Doherty et al., 2005). The advantage of the method compared to standard Monte-Carlo is that NSMC is able to generate many models, all respecting a user-specified objective function threshold (Eq. (1)) using at most a few PEST calibration iterations for each realization.

For the case presented in the current paper, the implementation of the NSMC method, combined with particle back-tracking, requires the following steps summarized in Fig. 5:

1) The first step of the NSMC method is to calibrate a single model; a parameter estimation was performed using the truncated singular value decomposition technique "SVD-assist" (Tonkin and Doherty, 2005), to minimize the objective function defined as

$$\varphi = \left(h - X\underline{p}\right)^T Q \left(h - X\underline{p}\right) \tag{1}$$

where h is the vector of observation data (only hydraulic head observations were available), X is the sensitivity matrix of the simulated data with respect to each parameter values, Q is the matrix of the squared observation weights, and $\underline{p}$ is the vector of current parameter values.

For SVD, the estimated parameter set $\underline{p}$ is given by the following equation expressed in terms of the resolution matrix R:

$$\underline{P} = Rp + G\varepsilon \tag{2}$$

where G is a matrix of a generalized inverse of X^TQX and ε expresses measurement noise. In the absence of the latter, the resolution matrix represents the estimated values of $\underline{p}$ as a weighted average of true parameters p multiplied by each row of R. In this context, a unique solution to the inverse problem is attainable.

2) Based on the calibrated deterministic model, it is possible to generate calibration-constrained parameter sets with high computational efficiency. A set of parameter realizations is generated with the PEST utility RANDPAR. From Eq. (2), parameter error can be expressed as follows:

$$(p - \underline{p}) = (I - R)p - G\varepsilon \tag{3}$$

where I is the Identity matrix. Since p is unknown, Eq. (2) cannot be solved but statistical properties of the parameter error can be computed as

$$C(p - \underline{p}) = (I - R)C(p)(I - R)^T + GC(\varepsilon)G^T \tag{4}$$

where $C(p)$ is the parameter covariance matrix that expresses the innate variability of the parameter based on knowledge of the properties,

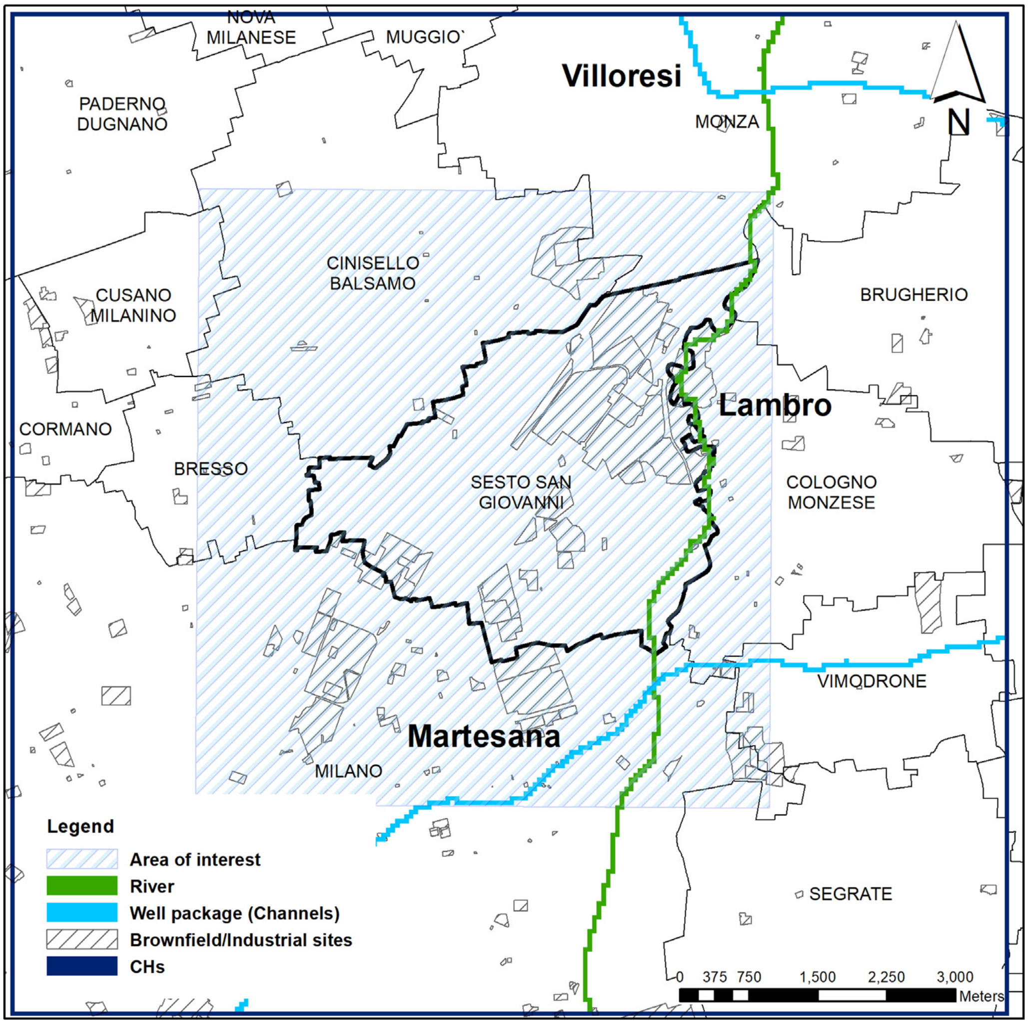

Fig. 4. Boundary Conditions and internal conditions: Constant head with-blue, river (green) and channels (light-blue) simulated with WELL package as losses).

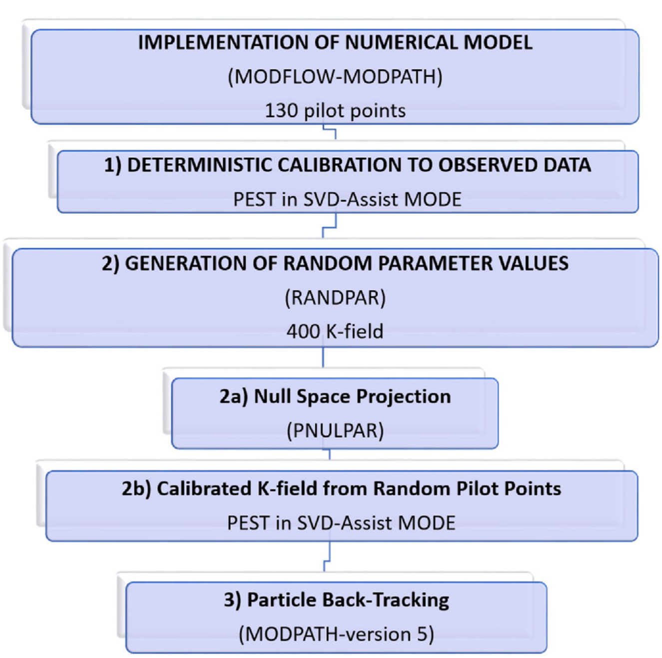

Fig. 5. Flowchart of the inverse iterative Null Space MONTECARLO

in this case on the variogram model. This equation is divided into two parts: the first term depends on the null-space component of p and expresses the loss of system details during the calibration process, while the second depends on the measurement noise of observations from which $\underline{p}$ is estimated.

2a) Using SVD for inversion, the difference between I and R is given by projection onto the null space, which is defined by

$$I - R = V_2 V_2^T \tag{5}$$

The right-hand side term of Eq. (5) is the calibration solution subspace used to project differences between stochastic parameter realizations generated using $C(p)$ and the calibrated parameter values onto the calibration null space as

$$(p - \underline{p_{st}})^T = V_2 V_2^T (p - \underline{p_{st}}) \tag{6}$$

where p_{st} represents the stochastic parameter values and the first term $(p - \underline{p_{st}})^T$, equals the projected parameter difference. Finally, the projected differences (projection in the null space can be undertaken using the PNULPAR utility) are added to the calibration parameters to generate new calibration parameter sets $\underline{p}$. Under most circumstances, this replacement will result in a slightly decalibrated model, depending on model non-linearities and on the fact that the cutoff between calibration solution and null space is not sharp (therefore, it does not correspond with the location of zero-valued singular values).

2b) Whether the model is decalibrated (i.e. the objective function is above a defined threshold), recalibration is effected, through the SVD-assist methodology (Doherty, 2015), by adjusting only the solution-space-parameter eigencomponents, which are the coefficients of vectors making up the matrix obtained from SVD of $\sqrt{Q}X$. This adjustment usually requires one or two PEST iterations (Doherty, 2015) that, using SVD-assist, have been undertaken, in the present case, with 20 Modflow model runs at most.

3) Using MODPATH, it is possible to advectively back-trace the particles, which originate in correspondence with the monitoring wells subjected to a diffuse contamination. A MODPATH simulation is undertaken for each model implemented using a random parameter hydraulic field (2b).

The NSMC method has a number of advantages that, together, can substantially improve the calibration-constrained stochastic parameter fields. For example, it is model-independent, it can be used with any type of model and it allows the setting of constraints in order to replicate observations of the system state.

2.1. Procedure overview of particle back-tracking under uncertainties

The flow chart in Fig. 6 shows in greater detail the previously described step (3), developed in this study in order to assess areas with a high occurrence frequency to be associated with a diffuse contamination.

Starting from each of the 400 generated stochastic K-fields, the following steps were undertaken:

Step 3a. For the i-th generated K-field, the monitoring wells whose monitored median PCE concentration values (time interval 2010–2014) exceeds the concentration of 10 μg/l, were considered as starting locations of each particle. As the PCE limit under the Italian drinking water standard is 10 μg/l, the choice to consider only points above this value was taken with a view to only focus on MPS responsible of a medium-high diffuse PCE contamination.

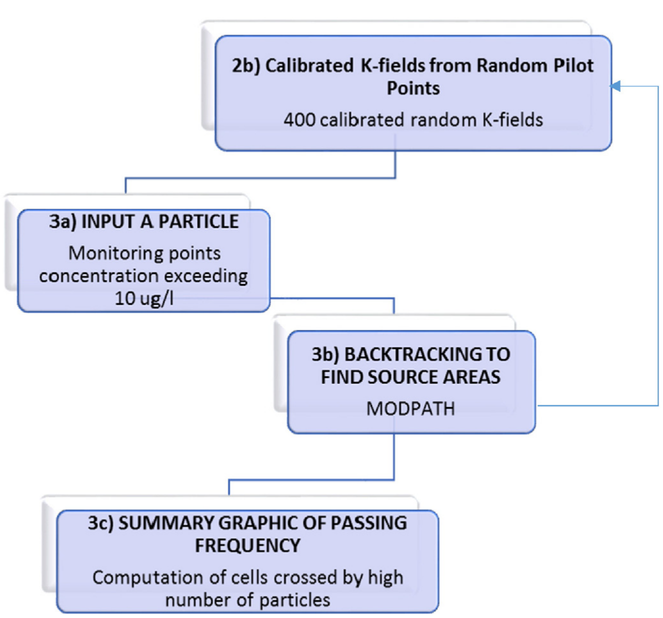

Fig. 6. Flow diagram of the Monte Carlo back-tracking using MODPATH.

Step 3b. Using MODPATH, a particle back-tracking was performed for each i-th K-field. This approach was chosen to simplify the solute transport process by considering only the advection. Dispersion, diffusion, decay and sorption were neglected because the aim of the methodology is neither to represent the concentration distribution in groundwater, nor to find the exact position of the sources. The simplified approach aims at identifying the most probable paths followed by groundwater contamination, which coincide with the groundwater flow directions. An alternative method that applies NSMC considering all the transport processes and the release of contaminant mass can be found in (Alberti et al., 2017), but its application is more complicated as it requires a transport model, which also takes a far higher simulation time compared to particle tracking.

Step 3c. At the end of the cycle, the total number of particles that passed through each model cell is summed for all the simulations. Alter-natively, particle end point analysis could be used considering that the source should be located where the particle enters the aquifer via recharge. However, for the pilot area studied here, it is known that in the past some industries used to directly discharge contaminated waste waters into the aquifer through deep-screened injection wells. Therefore, the particle count approach has been considered more suitable in identifying areas where MPS are most likely positioned. The result consists of a map for each aquifer layer highlighting the areas most frequently interested by the passage of particles, i.e. by con-taminated groundwater. These areas are considered as having the highest likelihood to host MPS responsible for the medium-high diffuse PCE contamination.

2.2. Stochastic model implementation for the pilot area

The parameterization of the model employed the pilot point technique to represent the spatial variability of horizontal hydraulic conductivity in Layers 1, 2, 3 (vertical hydraulic conductivity was tied to horizontal with a factor of 0.1). Pilot points parameterization of the model domain took into account two different levels. A regular grid was distributed uniformly with a separation distance of 2 km. This reg-ular grid was supplemented with individual pilot points in correspon-dence with pumping test, where the value of hydraulic conductivity could be considered with a low uncertainty. For purposes of random parameterization, the log for each pilot point was assigned in a range between lower ($1 \cdot 10^{-5}$ m/s) and upper ($1 \cdot 10^{-2}$ m/s) bounds based on expert knowledge (log-stratigraphy in pilot area). The pilot points representing wells subjected to pumping tests were assigned a very narrow range. A total number of 130 pilot points were used for the parameterization of hydraulic conductivity during NSMC procedure (Fig. 7). Assuming a normal distribution, the bounds for the log of each K pilot point (previously defined) were supposed to comprise the 95% confidence interval of the estimate.

The spatial structure of the log of hydraulic conductivity was described by an exponential variogram and the interpolation of the K-field calculated by PEST was done by ordinary kriging (in S4 an example of K distribution is represented). A number of 400 realizations were generated and then calibrated (for a total number of 20,970 Modflow model runs) using the NSMC approach already described. The deterministic calibrated model has a ϕ (See Eq. (1)) of 6.21, an Absolute Residual Mean (ARM) = 0.47 m, an ARM scaled on range of observations = 0.013 and a water balance error < 1%. It is generally acknowledged that the thresh-old objective function below which a model is deemed to be “calibrated” is somewhat subjective. In the present case study, models with a ϕ lower than 6.21 were obtained during calibration, although the high K heterogeneity of these models showed a potential overcalibration. The smoother K distribution of the deterministic calibrated model satisfies the need to avoid overcalibration while keeping the fit to measurements sufficiently low. Consequently, a ϕ of 6.21 was considered a sufficiently high threshold to give PEST the “room to move” to span the parameter space. Moreover, these calibration statistics were judged satisfactory by

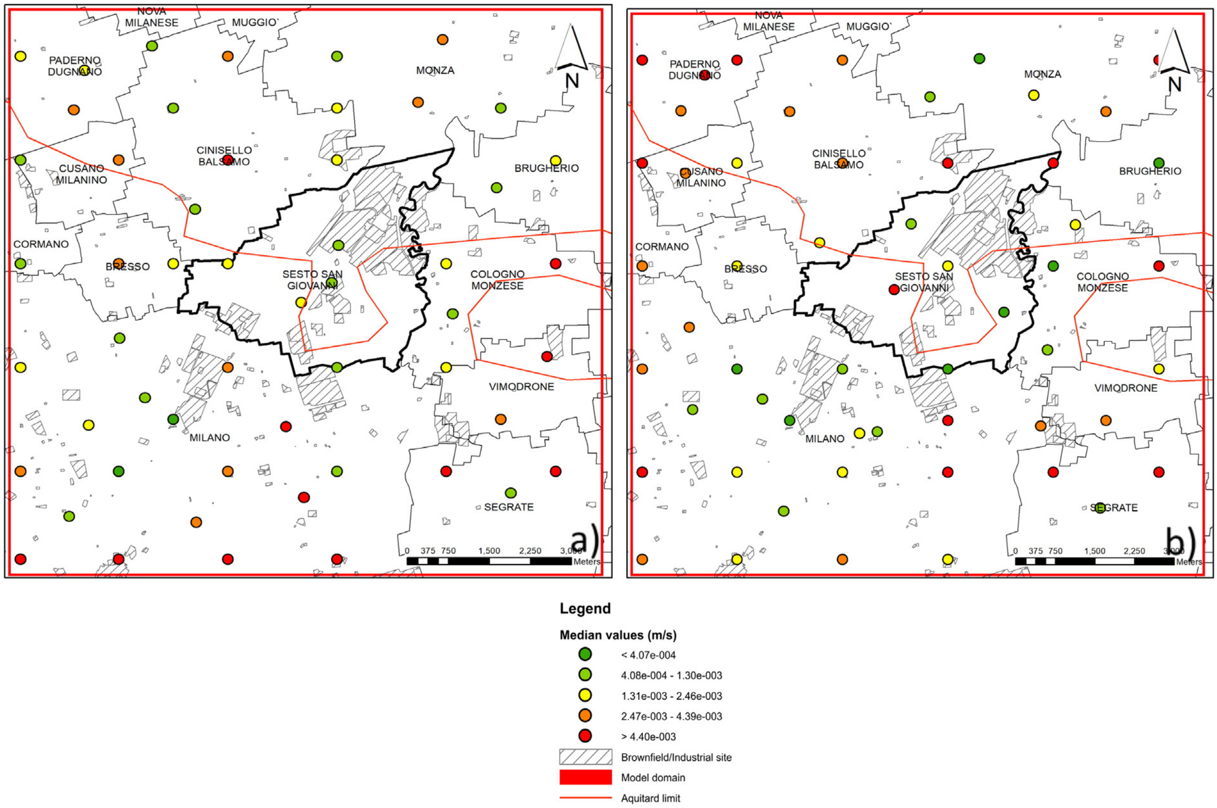

Fig. 7. Pilot point grid for a) Layer 1 and b) layer 3. The values represented are the median of the sampled distribution used during NSMC procedure.

public authorities for the modeling purposes; for this reason among the 400 models, only those with a final ϕ lower than 6.21 were retained; consequently, 11 models were discarded and the 389 models accepted have an ARM ranging between 0.36 and 0.47 m. Fig.8 shows the scatter-diagram of initial and final objective function: constrained-parameter calibration with NSMC allows to reduce the initial objective function.

Fig. 9 shows the interpolation map of standard deviation of log (K) in pilot points. The values are in line with the range of reasonable values, as defined for every pilot point on the basis of geological knowledge and pumping test interpretation. In other words, the uncertainty in parameter values is adequately represented by the sampled values and areas with a low variation (green zones in Fig. 9) mainly correspond to those pilot points having narrow boundaries based on available pumping test results.

The calibration dataset consists of head measurements monitored during the piezometric campaign in May 2014. A total of 63 head targets were placed in Layer 1 (50 points) and Layer 3 (13 points) (Fig.10) based on the well screen depths.

The 389 calibrated models were used to backtrack particles from the monitoring wells showing a median PCE value higher than 10 μg/l, that corresponds to 41 final locations (red and violet dots in Fig. 2). In most cases, PCE concentrations were collected from monitoring wells with an

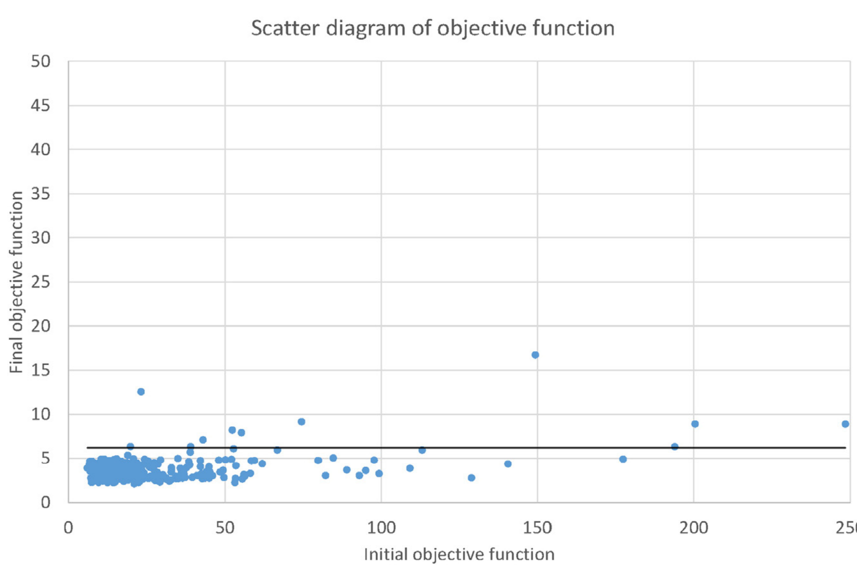

Fig. 8. Scatter diagram for the 400 k-fields. Only 11 simulations were excluded because ϕ is higher than 6.21 objective function (black line) of deterministic calibrated model.

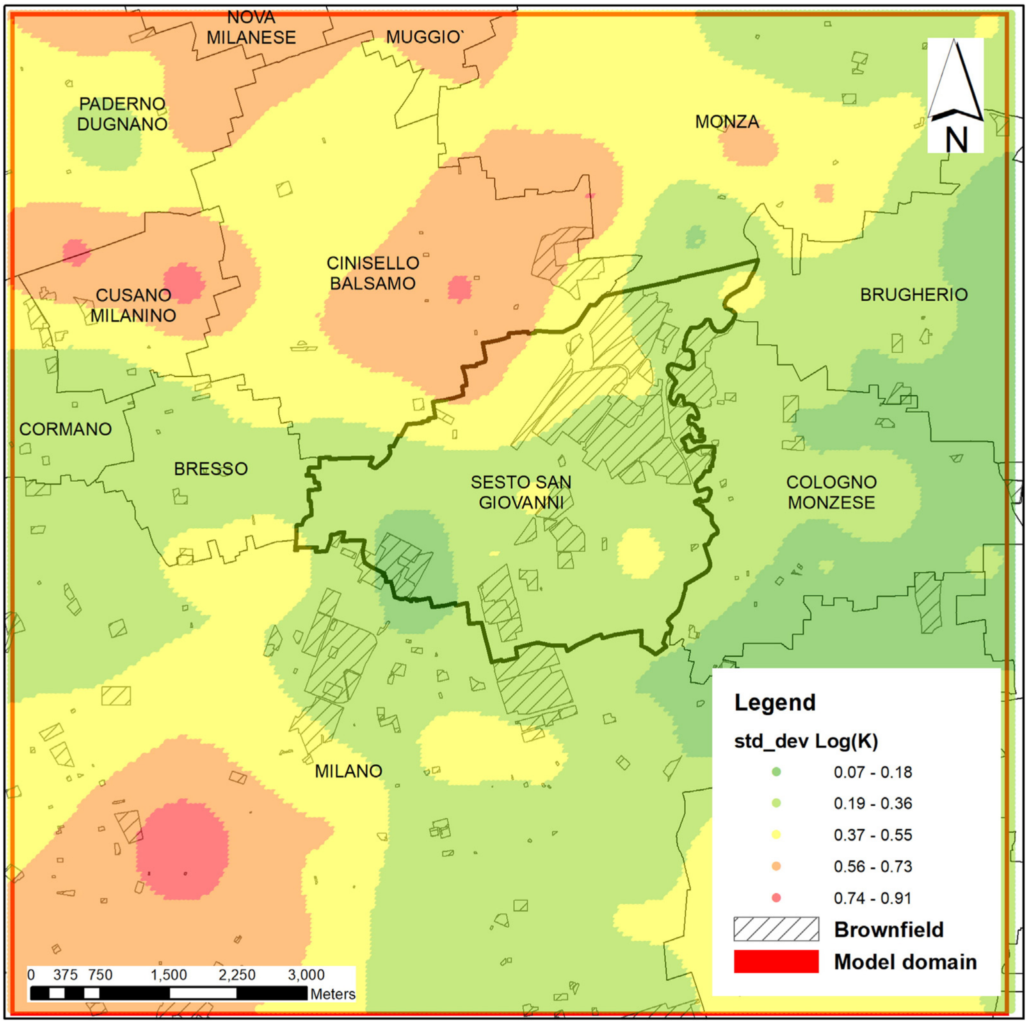

Fig. 9. Map of standard deviation of Log (K) on a cell by cell basis; a value of 1 means a variation of an order of magnitude in K values.

identified well stratigraphic log reporting the screen depth. As particle back-tracking analysis is sensitive to the starting depths of the particles, the assignment of their starting locations was based on the actual screen position. For each well, a particle was added at the center of the screened depth for each layer crossed by the screen length (e.g. if the well screens cross all three layers, 3 particles were added, one in each layer). Considering the uncertainty associated with the hydraulic conductivity value, the direction of the simulated pathlines differed for the same particle starting locations because of different K-fields generated with the NSMC procedure. By computing the number of particles crossing every model cell in all the 389 simulations, it is possible to obtain maps (Fig. 11 and Fig. 12) of occurrence frequency of the particle traveling in each aquifer layer (i.e. Layer 1 and Layer 3).

3. Results and discussion: particle back-tracking under NSMC procedure

For cells with a high frequency, the simulated particle tracking outlined the approximate area that contributed to a diffuse PCE contamination exceeding the legal drinkable water limit. Multiple Point Sources of PCE might contribute to the observed contamination in wells if they are located anywhere along the particle pathlines. The representation in maps and the interpretation of results can be difficult in areas where the particle pathlines overlap. For this reason, in the present paper the resulting pathlines have been grouped based on the location of well screen (Aquifer A or Aquifer B). Fig. 11 displays, for each model cell, the particle occurrence frequency for the particles starting in Aquifer A (Layer 1). In this case, particles flow in Layer 1 only, because in the backtrack path they progressively move toward the water table. Orange and red colors identify zones (strips) having an occurrence frequency higher than 50% and consequently a higher probability to host MPS responsible of the medium-high diffuse contamination (i.e. >10 μg/l) detected in the area of interest. For the sake of simplicity, in the following figures the areas where MPS are most likely positioned are indicated with numbers and letters (e.g. "1A" refers to area 1 in Aquifer A). The highest frequencies (>75%) are found in the central area of Sesto San Giovanni (2A) and near the border between the latter and Brugherio (3A).

In Fig. 12, the particle occurrence frequency for particles starting in layer 3 is represented; in this case some particles, mainly those placed North to the aquitard limit, move backward while decreasing the depth and partially flowing into Layer 1. Also, in this map, some areas having an occurrence frequency higher than 50% have been identified. It is interesting to note that wells pertaining to the public water supply of "Centrale Gorla" are hit by a diffuse contamination caused by MPS falling into the strip identified with the code 1B, which has a long N—S extension but a small width (<500 m). Furthermore this strip overlaps with the strip (1A) identified in Layer 1, showing that the MPS responsible of the diffuse contamination can be the same for both aquifers. A similar situation occurs in the central sector of Sesto San Giovanni, where the monitoring wells in Layer 3 are subjected to a diffuse contamination coming from MPS likely positioned in a narrow

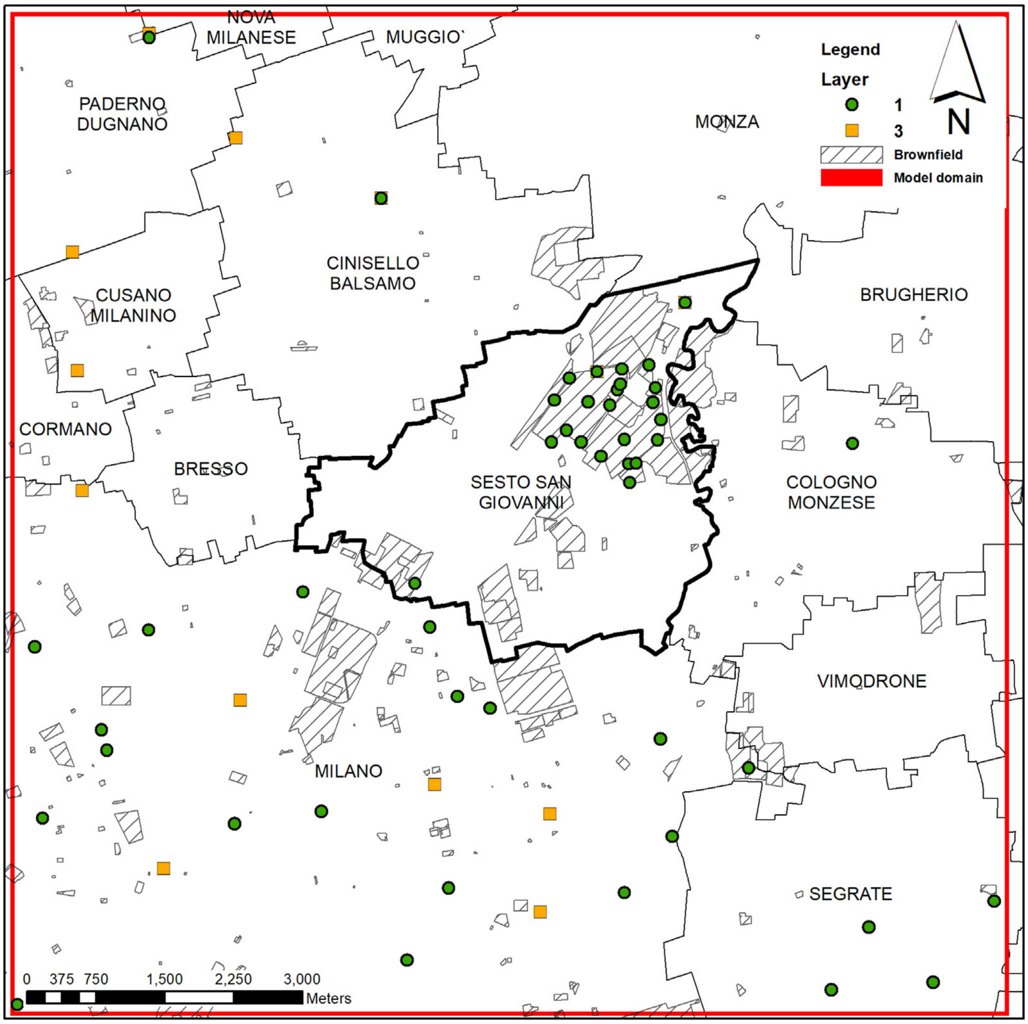

Fig. 10. Monitoring wells where heads were measured in May 2014. Points represent the heads representative of the Layer 1, whereas the squares ones are representative of the Layer 3.

strip (<250 m, 3B) that overlaps with the strip (2A). Differently the strip (2B) is not overlapping with any strip in Layer 1, although the small number of monitoring wells screened in this Layer affects the reliability of this result. Finally, the strip (4B) shows only cells having a frequency lower than 50%, indicating that MPS linked to (3A) likely influence groundwater quality in Layer 3 because the particles starting in Layer 3 (that in this part of the model represents the deepest part of the unseparated aquifer) flow back to the immediate upgradient portion in Layer 1.

In the present paper, the only parameter subjected to variation within the NSMC approach has been the distribution of hydraulic conductivity. Whereas other parameters could be taken into account, limiting the number of parameters enabled attention to focus on evaluating the potential of this method while keeping the procedure manageable.

For the Milano's FUA considered here, future applications of the method should take into account all the potential sources of uncertainty related to contaminant flow paths (e.g. BC, recharge, river water exchanges). As an illustrative example, the paths resulting from the application of different perimeter boundary heads (Haitjema, 1995), which represent water level conditions observed in previous years (from 2008 to 2013), were calculated. Although, for the study area here considered, the spread of the different particle paths starting from the center of the model is limited, the example shows how, in the model domain, other sources of uncertainty can affect the flow paths, suggesting that in some cases, the high-probability areas may actually be wider than assessed by the above NSMC results.

The Fig. 13 shows that varying the BCs doesn't affect the results in the central part of the model, as particle backtracked paths still lie with-in the area identified by varying the conductivities. Differently in the Eastern and Western parts of the model (outside the area of interest and hence not represented in the maps), an influence on the flow path is more pronounced and it is linked to the variability of the main flow direction. Future exercises could assess the uncertainty related to more than one parameter, such as BCs (Fig. 13), recharge and conduc-tance of internal conditions as follows:

- BCs: it is suggested to consider BCs as part of the NSMC simulations, considering for example a distribution or a variance of flow directions based on a representative time span of piezometric surveys; by sampling different flow directions (i.e within a GIS platform), it could be possible to explore the variability of the path due to different BCs realizations.
- Recharge: many authors (Baalousha, 2016a, 2016b) considered uncertainty analysis by sampling the distribution of a dataset of infiltration rates spanning many years.
- Internal boundary conditions: the variability of the conductance of river and channels could be sampled within the NSMC procedure (Juckem et al., 2014).

In addition, it must be noted that results obtained with the proposed methodology can be influenced by the distribution of the monitoring wells. This is mainly true when the clustered monitoring wells are

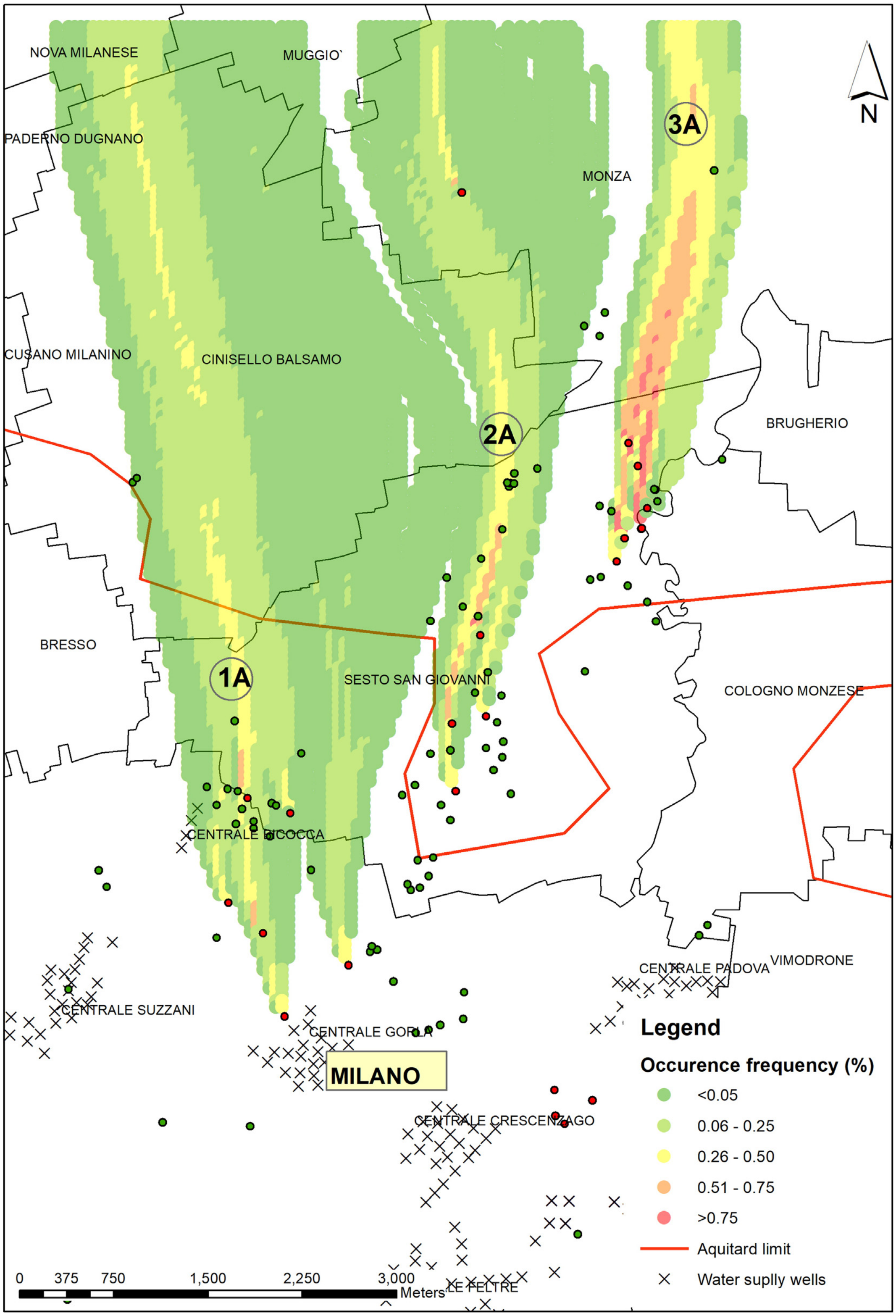

Fig. 11. Contributing areas (Layer 1-Aquifer A) defined by frequency occurrence of particle backtracking for 389 models. All areas are circumscribed by particle pathways outlining the areal extent of the zone of contribution to diffuse contamination for a group of 16 groundwater sampling locations in northern Milan having a median concentration > 10 μg/l recognized by Regione Lombardia as a diffuse contamination.

positioned along the average groundwater flow direction: in this case, the number of particle passages is summed along that direction, such as along strip 3A. On the other hand, clustered monitoring wells placed orthogonal to groundwater flow direction don't influence the results because particles for each K-field would move mainly parallel to each other, thus not summing up, such as in strip 2B. Only a regular monitor-ing well grid (impossible to have in such a huge area as the study area) would prevent the influence of groundwater sampling deriving from clustered monitoring wells. The methodology proposed has the advantage that maps showed in Fig. 11 and Fig. 12 are reporting all the starting

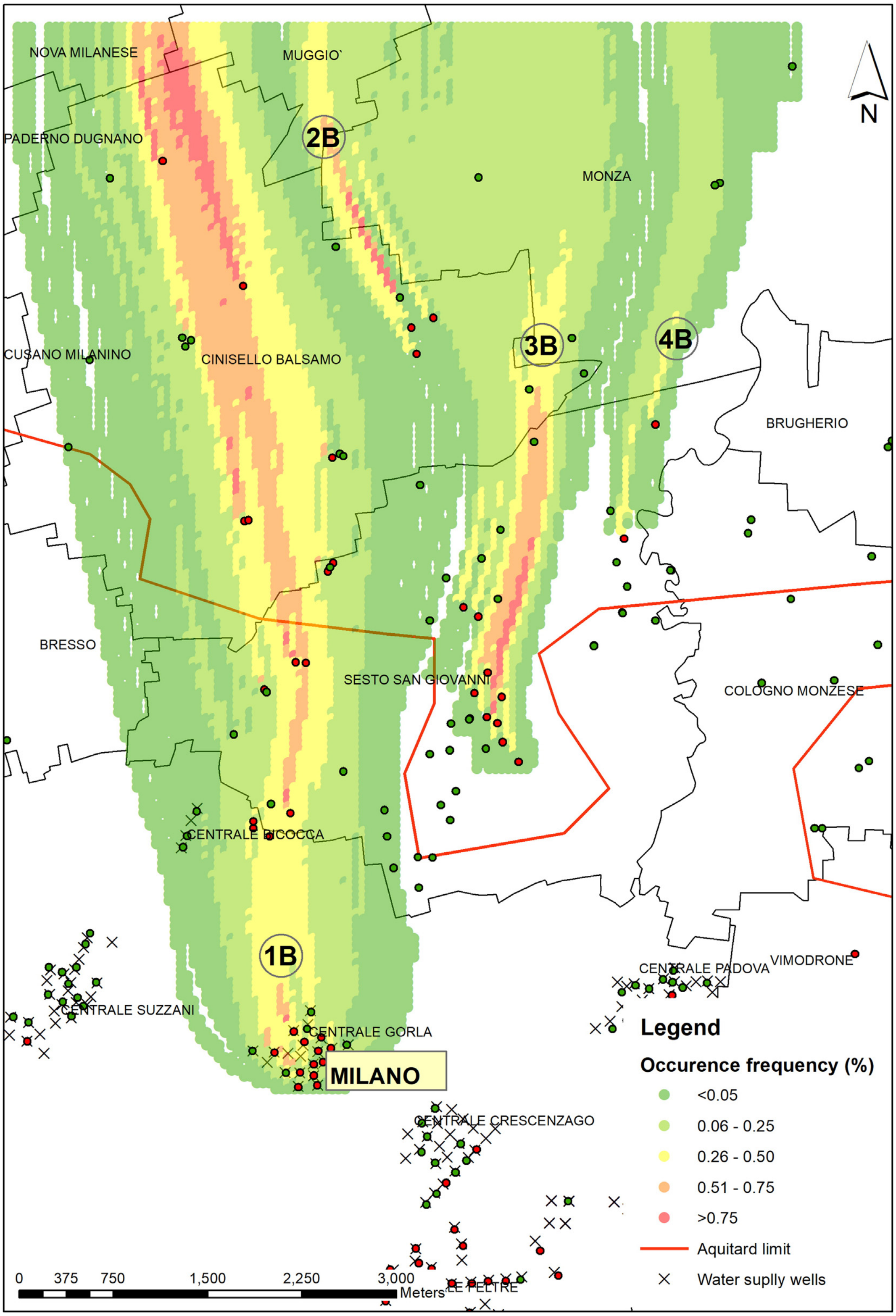

Fig. 12. Contributing areas (Layer 3-Aquifer B) defined by frequency of particle backtracking for 389 models. All areas are circumscribed by particle pathways outlining the areal extent of the zone of contribution to diffuse contamination for a group of 25 groundwater sampling locations in northern Milan having a median concentration > 10 μg/l recognized by Regione Lombardia as a diffuse contamination.

points of each particle, thus, they show all the necessary information to interpret the results. Nevertheless, in order to reduce the effect of sampling positions future research would need to evaluate the opportunity to apply geometric methods (e.g, a buffer surrounding the points) or a weight method (e.g. placing more particles at isolated wells).

4. Conclusions

The anthropogenic diffuse contamination in urban areas is a challenging problem that requires new tools able to support Public Authorities in planning their activities. This paper is presenting a new

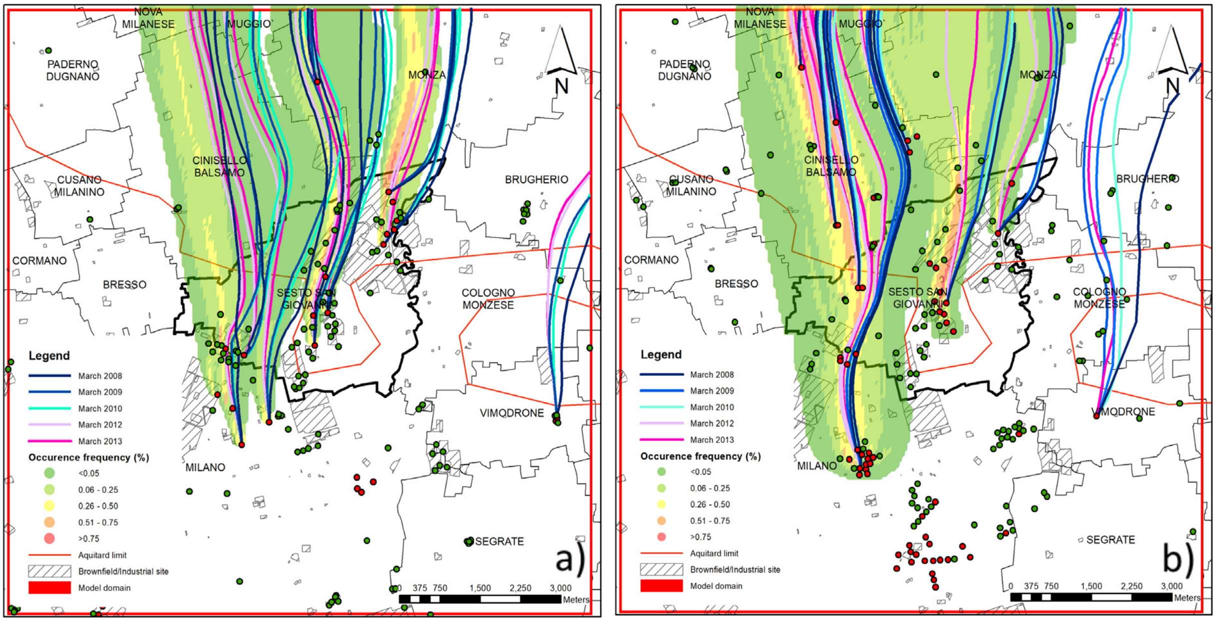

Fig. 13. Contributing areas a) Layer 1-Aquifer A and b) Layer 3-Aquifer B defined by frequency occurrence of particle backtracking for 389 models and superposition of particle pathlines backtracking (with continuous line) given boundary heads from 2008 to 2013 heads surveys.

approach, based on numerical modeling, devoted to identify areas with the highest likelihood to host potential Multiple Point Sources (MPS) responsible of a diffuse contamination.

The methodology has been applied in the N-E sector of the Milan Functional Urban Area, where a PCE diffuse contamination has been acknowledged by Regional Authorities. In order to address the uncertainty related to the sources contributing to PCE diffuse contamination, a 3D groundwater flow model was implemented. After-wards, a Null-Space Monte Carlo inverse modeling procedure was applied to generate 389 models, each characterized by a different distribution of hydraulic conductivity but all of them respecting the constraint of a good fit to calibration head measurements. Back-tracking, for each realization, the path of particles that start from contaminated monitoring wells and computing for each model cell the number of particle passages, it has been possible to produce maps representing the particle occurrence frequency. The value of these maps is to show the areal extent of the zones (strips) that most probably contain MPS responsible of the detected PCE diffuse contamination. Each cell contained in the strips should be considered as a potential area of PCE release, with a high probability (>75%) for the red cells and a low probability (<25%) for the green ones (see Fig. 11 and Fig. 12). The uncertainty predictive analysis will help Public Authorities to optimize public economic resources by planning investigations preferentially in those areas that are likely responsible for the diffuse contamination. Furthermore, the results of the stochastic methodology highlight areas where the FUA monitoring network should be improved to better survey the fate of diffuse contamination. Finally, the management of pumping for public use can also be improved if the upgradient presence of MPS clusters is accounted for.

For the present study, the methodology has been successfully applied to PCE contamination considering only the uncertainty linked to the distribution of hydraulic conductivity. Actually, there are no limitations to the application to any other chemicals whose presence in groundwater has been recognized as being linked to a diffuse contamination. Future research developments should consider a higher number of parameters to increase the exploration of the uncertainty linked to the hydrogeological properties.

Acknowledgments

This study was supported by the EU AMIIGA Project (Interreg Central CE32) (AMIIGA-Nr° CE32).

The authors thank Regione Lombardia and ARPA for their support during data collection. The authors are also grateful to John Doherty for being available in discussing NSMC application and for his advices. The authors would like to thank Daniel Feinstein (U. S. Geological Survey-Wisconsin) for the revision of the PhD thesis of Loris Colombo that concerns diffuse contamination and NSMC applications.

Appendix A. Supplementary data

Supplementary data to this article can be found online at https://doi. org/10.1016/j.scitotenv.2017.11.253.

References

Alberti, L., Francani, V., 2001. Studio idrogeologico sulle cause del sollevamento della falda nell'area milanese. Geoing. Ambient. e Mineraria 104, 257–264.

Alberti, L., Bianchi, D., Ceccon, S., 2003. The implementation of a flux model for the appli-cation of groundwater integrated management. Int. J. River Basin Manag. 1. https://doi.org/10.1080/15715124.2003.9635200.

Alberti, L., Lombi, S., Zanini, A., 2011. Identifying sources of chlorinated aliphatic hydrocarbons in a residential area in Italy using the integral pumping test method. Hydrogeol. J. 19. https://doi.org/10.1007/s10040-011-0742-1.

Alberti, L., Colombo, L., Francani, V., 2014. The groundwater flow velocity distribution in the urban areas: a case study. Ital. J. Eng. Geol. Environ. 14. https://doi.org/10.4408/IJEGE.2014-02.O-02.

Alberti, L., Cantone, M., Colombo, L., Oberto, G., La Licata, I., 2016. Assessment of aquifers groundwater storage for the mitigation of climate change effects. Rend. Online Soc. Geol. Ital. 39:89–92. https://doi.org/10.3301/ROL.2016.54.

Alberti, L., Azzellino, A., Colombo, L., Lombi, S., 2016a. Use of cluster analysis to identify tetrachloroethylene pollution hotspots for the transport numerical model implemen-tation in urban functional area of Milan, Italy. International Multidisciplinary Scientif-ic GeoConference Surveying Geology and Mining Ecology Management. SGEM https://doi.org/10.5593/SGEM2016/B11/S02.091.

Alberti, L., Cantone, M., Colombo, L., Lombi, S., Piana, A., 2016b. Numerical modeling of regional groundwater flow in the Adda-Ticino Basin: advances and new results. Rend. Online Soc. Geol. Ital. 41. https://doi.org/10.3301/ROL.2016.80.

Alberti, L., Colombo, L., Formentin, G., Oberto, G., 2017. Assessment of sources of PCE con-tamination in groundwater using a Monte Carlo method in the functional urban area of Milano. Rend. Online Soc. Geol. Ital. 42. https://doi.org/10.3301/ROL.2017.15.

ARPA Lombardia, 2015. PROGETTO PLUMES: Final Report.

ARPA Lombardia, 2016. PROGETTO PLUMES - Final Report.
Baalousha, H.M., 2016a. Using Monte Carlo simulation to estimate natural groundwater recharge in Qatar. Model. Earth Syst. Environ. 2, 87. https://doi.org/10.1007/s40808-016-0140-8.
Baalousha, H.M., 2016b. Development of a groundwater flow model for the highly parameterized Qatar aquifers. Model. Earth Syst. Environ. 2, 67. https://doi.org/10.1007/s40808-016-0124-8.
Bard, Y., 1974. Nonlinear parameter estimation. Oper. Res. Q. 19701977. https://doi.org/10.1016/j.ultras.2008.11.002.
Bauer, S., Bayer-Raich, M., Holder, T., Kolesar, C., Müller, D., Ptak, T., 2004. Quantification of groundwater contamination in an urban area using integral pumping tests. J. Contam. Hydrol. 75:183–213. https://doi.org/10.1016/j.jconhyd.2004.06.002.
Bayer-Raich, M., Jarsjö, J., Liedl, R., Ptak, T., Teutsch, G., 2006. Integral pumping test analyses of linearly sorbed groundwater contaminants using multiple wells: inferring mass flows and natural attenuation rates. Water Resour. Res. 42. https://doi.org/10.1029/2005WR004244.
Beven, K., Binley, A., 1992. The future of distributed models: model calibration and uncertainty prediction. Hydrol. Process. 6:279–298. https://doi.org/10.1002/hyp.3360060305.
Bini, A., 1997. Stratigraphy, chronology and paleogeography of Quaternary deposits of the area between the Ticino and Olona rivers (Italy-Switzerland). Geol. Insubrica 2, 21–46.
Carcano, C., Piccin, A., 2002. Padans Aquifer Geology of the Lombardy Plain. Firenze.
Carrera, J., Neuman, S.P., 1986. Estimation of aquifer parameters under transient and steady state conditions: 2. Uniqueness, stability, and solution algorithms. Water Resour. Res. 22:211–227. https://doi.org/10.1029/WR022i002p00211.
Carrera, J., Alcolea, A., Medina, A., Hidalgo, J., Slooten, L.J., 2005. Inverse problem in hydrogeology. Hydrogeol. J. https://doi.org/10.1007/s10040-004-0404-7.
Christensen, S., Cooley, R.L., 1996. Simultaneous confidence intervals for a steady-state leaky aquifer groundwater flow model. Calibration and Reliability in Groundwater Modelling, pp. 561–569.
Citarella, D., Cupola, F., Tanda, M.G., Zanini, A., 2015. Evaluation of dispersivity coefficients by means of a laboratory image analysis. J. Contam. Hydrol. 172:10–23. https://doi.org/10.1016/j.jconhyd.2014.11.001.
Doherty, J., 2010. Methodologies and software for PEST-based model predictive uncertainty analysis. Bericht 33.
Doherty, J., 2014. Addendum to the PEST manual. PEST Man. Add. 313.
Doherty, J.E., 2015. Calibration and Uncertainty Analysis for Complex Environmental Models - PEST: Complete Theory and What it Means for Modelling the Real World.
Doherty, J., Welter, D., 2010. A short exploration of structural noise. Water Resour. Res. 46. https://doi.org/10.1029/2009WR008377.
Doherty, J., Brebber, L., Whyte, P., 2005. PEST: Model-independent Parameter Estimation. Vol. 122. Watermark Comput, Corinda, Aust. https://doi.org/10.1016/B978-141600119-5.50003-2.
Draper, N.R., Smith, H., 1981. Applied Regression Analysis. Applied Regression Analysis, p. 709.
European Environment Agency, 2013. Annual Report 2012 and Environmental Statement 2013. Vol. 100.
European Union, 2006. Directive 2006/118/EC of the European Parliament and of the council of 12 December 2006 on the protection of groundwater against pollution and deterioration. Off. J. Eur. Union 19:19–31 doi:http://eur-lex.europa.eu/legal-con-tent/EN/TXT/?uri=CELEX:32006L0118.
Fasolini, D., Zini, E., 2014. Rappoorto sulla consistenza del suolo agricolo e sue variazioni. Francani, V., Beretta, G. Pietro, 1995. Preliminary Survey about Sustainable use of Deeper
Groundwater in Milano Province. Milan.
Frumkin, H., 2002. Urban sprawl and public health. Public Health Rep. 117:201–217. https://doi.org/10.1016/S0033-3549(04)50155-3.
Gattinoni, P., Scesi, L., 2017. The groundwater rise in the urban area of Milan (Italy) and its interactions with underground structures and infrastructures. Tunn. Undergr. Sp. Technol. 62. https://doi.org/10.1016/j.tust.2016.12.001.
Guadagnini, A., Neuman, S.P., 1998. Deterministic solution of stochastic groundwater flow equations by nonlocal finite elements. Comput. Methods Contam. Remediat. Water Resour. 12, 347–354.
Haitjema, H.M., 1995. Analytic element modeling of groundwater flow. Anal. Elem. Model. Groundw. Flow:203–305 https://doi.org/10.1016/B978-012316550-3/50005-2.
Harbaugh, B.A.W., Banta, E.R., Hill, M.C., Mcdonald, M.G., 2000. MODFLOW-2000, The U.S. Geological Survey Modular Ground-water model — User Guide to Modularization Concepts and the Ground-water Flow Process. U.S. Geological Survey.
Harvey, C.F., Gorelick, S.M., 1995. Temporal moment-generating equations - modeling transport and mass-transfer in heterogeneous aquifers. Water Resour. Res. 31, 1895–1911.
Herckenrath, D., Langevin, C.D., Doherty, J., 2011. Predictive uncertainty analysis of a salt-water intrusion model using null-space Monte Carlo. Water Resour. Res. 47. https://doi.org/10.1029/2010WR009342.
Juckem, P.F., Fienen, M.N., Hunt, R.J., 2014. Simulation of Groundwater Flow and Interaction of Groundwater and Surface Water on the Lac du Flambeau Reservation, Wiscon-sin. U.S. Geological Survey.
Kuroda, K., Fukushi, T., 2008. Groundwater contamination in urban areas. Groundw. Manag. Asian Cities; cSUR-UT Ser. Libr. Sustain. Urban Regen:pp. 125–149 https://doi.org/10.1007/978-4-431-78399-2_7.
Moore, C., Doherty, J., 2005. Role of the calibration process in reducing model predictive error. Water Resour. Res. 41:1–14. https://doi.org/10.1029/2004WR003501.
Nolan, B.T., Hitt, K.J., Ruddy, B.C., 2002. Probability of nitrate contamination of recently recharged groundwaters in the conterminous United States. Environ. Sci. Technol. 36:2138–2145. https://doi.org/10.1021/es0113854.
Pedretti, D., Fernàndez-Garcia, D., Bolster, D., Sanchez-Vila, X., 2013. On the formation of breakthrough curves tailing during convergent flow tracer tests in three-dimensional heterogeneous aquifers. Water Resour. Res. 49:4157–4173. https://doi.org/10.1002/wrcr.20330.
Perego, R., Bonomi, T., Fumagalli, M.L., Benastini, V., Aghib, F., Rotiroti, M., Cavallin, A., 2014. 3D reconstruction of the multi-layer aquifer in a Po plain area. Rend. Online Soc. Geol. Ital. 30:41–44. https://doi.org/10.3301/ROL.2014.09.
Pollock, D.W., 1994. User's guide for MODPATH/MODPATH-PLOT, Version 3: a particle tracking post-processing package for MODFLOW, the U.S. Geological Survey finite-difference ground-water flow model. Open-File Rep 94-464 0–249. doi:94-464.
Pollock, D.W., 2012. User guide for MODPATH version 6—a particle-tracking model for MODFLOW. Sect. A, Groundw. B. 6, Model. Tech 58 p. https://doi.org/10.3133/ofr20161086.
Provincia di Milano, 1992. Indagini sulla presenza di composti organo-alogenati nelle acque di falda della Provincia di Milano. Milano.
Rumbaugh, J.O., Rumbaugh, D.B., 2014. Using MODHMS with Groundwater Vistas Version 6. Environmental Simulations, Inc All Rights Reserved, Reinholds, PA 17569.
Stevenazzi, S., Masetti, M., Nghiem, S.V., Sorichetta, A., 2015. Groundwater vulnerability maps derived from a time-dependent method using satellite scatterometer data. Hydrogeol. J. 23:631–647. https://doi.org/10.1007/s10040-015-1236-3.
Stevenazzi, S., Masetti, M., Beretta, G. Pietro, 2017. Groundwater vulnerability assessment: from overlay methods to statistical methods in the Lombardy Plain area. Acque Sotter. Ital. J. Groundw. 6. https://doi.org/10.7343/as-2017-276.
Thornthwaite, C.W., Mather, J.R., 1955. The water balance. Publ. Climatol. 8, 1–104.
Tonkin, M.J., Doherty, J., 2005. A hybrid regularized inversion methodology for highly parameterized environmental models. Water Resour. Res. 41. https://doi.org/10.1029/2005WR003995.
Tonkin, M., Doherty, J., 2009. Calibration-constrained Monte Carlo analysis of highly parameterized models using subspace techniques. Water Resour. Res. 45. https://doi.org/10.1029/2007WR006678.
Troutman, B.M., 1985. Errors and parameter estimation in precipitation-runoff modeling: 1. Theory. Water Resour. Res. 21:1195–1213. https://doi.org/10.1029/WR021i008p01195.
Zhang, Y., Schaap, M.G., Guadagnini, A., Neuman, S.P., 2016. Inverse modeling of unsaturated flow using clusters of soil texture and pedotransfer functions. Water Resour. Res. 52. https://doi.org/10.1002/2016WR019016.